# Aerobic exercise during exposure to 40Hz light flicker protects against early cognitive impairments in Alzheimer's disease of 3xTg mice

**Sang-Seo Park**
Kyung Hee University School of Medicine
**Hye-Sang Park**
Kyung Hee University School of Medicine
**Chang-Ju Kim**
Kyung Hee University School of Medicine
**Seung-Soo Baek**
Sangmyung University
**Tae-Woon Kim** ( twkim0806@naver.com )
Sangmyung University https://orcid.org/0000-0001-8832-0874

**Research article**

**Keywords:** Alzheimer's disease, cognitive function, 40-Hz light flicker, exercise, amyloid-β, hippocampus, neuroplasticity, neurinflammation

**Posted Date:** November 3rd, 2020

**DOI:** https://doi.org/10.21203/rs.3.rs-100200/v1

# Abstract

**Background:** Alzheimer's disease (AD) is a progressive degenerative brain disease and the primary cause of dementia. At an early stage, AD is generally characterized by memory impairment involving recent experiences owing to dysfunctions of the cortex and hippocampus. The lesion gradually spreads to the association cortex. Early amyloid-β (Aβ) deposition and tau protein expression result in a loss of synaptic function, mitochondrial damage, and increased cell death via microglia and astrocyte activation, which ultimately lead to cognitive decline. Exercise has been identified as a powerful tool for preventing AD-related neuroinflammation and cognitive decline, and light flickering at 40 Hz light flicker is known to stabilize gamma oscillations and reduce Aβ. Therefore, we investigated whether exercise under 40-Hz light flickering protects against cognitive decline based on analyses of neuroinflammation, mitochondrial function, and neuroplasticity in the hippocampus in a 3xTg AD mouse model.

**Methods:** Using a 3xTg-AD model, 5-month-old mice were subjected to 12 weeks of exercise treatment and 40-Hz light flickering independently and in combination. Various factors, including spatial learning and memory, long-term memory, hippocampal Aβ, tau, neuroinflammation, pro-inflammatory cytokine expression, mitochondrial function, and neuroplasticity, were analyzed.

**Results:** Aβ and tau proteins levels were significantly reduced in the early stage of AD, resulting in protection against cognitive decline by reduced neuroinflammation and pro-inflammatory cytokines, improved mitochondrial function, reduced apoptosis, and increased synapse-related protein expression. In particular, exercise under 40-Hz light flickering was more effective than exercise or 40-Hz light flickering alone, resulting in improvements in parameter values to levels in the non-transgenic aged-match control group.

**Conclusions:** In this study, exercise under a special environment, such as 40-Hz light flickering, may exert a protective effect against cognitive decline. We detected synergistic effects of exercise and 40-Hz light flickering on pathological changes in the hippocampus in the early cognitive impairment of AD.


# Background

Alzheimer's disease (AD) is a progressive degenerative brain disease and the primary cause of dementia. In early AD, memory impairment, affecting the ability to recall recent experiences, results from cortex and hippocampal dysfunction. The lesion gradually spreads, primarily to the association cortex, thereby impairing overall cognitive function. The pathology of AD includes amyloid-β (Aβ) accumulation from amyloid plaques, tau aggregation by nerve fiber entanglement, and brain atrophy owing to a loss of neurons and synapses [1]. This supports the amyloid cascade hypothesis, which proposes that changes in Aβ initiate AD, and a series of events, including the accumulation of a toxic form of tau, triggers downstream neuronal death [2, 3]. Aβ deposition and tau protein expression ultimately result in cell death owing to a loss of synaptic function, mitochondrial damage, and microglia and astrocyte activation [4]. This hypothesis is strongly supported by the genetics of familial AD and the molecular basis of disease-

causing Aβ production and aggregation and the pathological accumulation of Aβ deposits beginning several years before the onset of symptoms. In addition to changes in Aβ, loss of synapses in early AD causes cognitive decline and tracks disease progression [1, 5]. The activation of microglia and astrocytes around amyloid plaques contributes to AD-related inflammation [6]. Neuroinflammation generally includes the release of reactive oxygen species (ROS), nitric oxide, pro-inflammatory chemokines, and cytokines and potentially includes the release of neurotoxin molecules from activated glia [7]. The overexpression of these mediators induces nerve damage in AD and other neurodegenerative disorders by various mechanisms [8]. Furthermore, the early stage of AD is associated with decreased mitochondrial function and oxidative damage [9]. Mitochondria are essential organs for the normal functioning of neurons, including synapse activation, and mitochondrial dysfunction is related to neurodegenerative diseases [10–12]. Given the important role of mitochondrial dynamics in neurons and the fact that morphological abnormalities of mitochondria are common pathological changes observed in AD, mitochondrial abnormalities are likely to be a common pathway leading to critical neurological dysfunction in the development of AD [12–15]. As such, excessive production of Aβ or plaque deposition causes cognitive impairment owing to nerve damage and loss in various areas of the brain.

Although various AD treatments are currently under development, there are still challenges. Many studies have shown that exercise has a positive effect on brain function. In various age groups, exercise is associated with a reduced risk of cognitive impairment in later life [16] and has a strong effect on neuroinflammation and cognitive decline in AD [17]. Exercise elicits a whole-body response involving metabolism and immunity [18]. Despite these findings, the beneficial effects of exercise are limited to either a delay or reduction in cognitive decline, rather than a complete improvement in cognitive function in AD. Accordingly, additional treatments are needed to complement the effects of exercise. It has recently been reported that various non-invasive gamma stimuli, such as 40-Hz light flicker and auditory stimuli, improve AD-related pathological factors and cognitive function [19–21]. Therefore, using a 6-month-old 3xTg-AD mouse model, we investigated the combined effects of aerobic exercise under 40-Hz light flicker on cognitive function and related pathological factors in the early stage of AD.

# Methods

## Animals

Mice were kept under the following conditions: arbitrary adjustment of food and water, 25 ± 1 °C, and light from 7 am to 7 pm. Mice were randomly divided into a wild-type (CON) group, 3xTG-AD (AD) group, 3xTg-AD and 40-Hz light flicker (AD + 40) group, 3xTg-AD and exercise (AD + EX) group, and 3xTg-AD and exercise with 40-Hz light flicker (AD + 40 + EX) group (n = 10 per group). All test animals were 5 months of age. The genotype of each animal was confirmed by a PCR analysis of DNA from tail biopsies. BrdU (Sigma, St. Louis, MO, USA) was administered intraperitoneally (i.p.) at 100 mg/kg/day for 7 days for 4 weeks prior to killing the animal to observe neurogenesis.

## Exercise protocol and exposure to 40-Hz light flickering

Exercise sessions were initiated in 5-month-old 3xTg mice. Animals in the exercise groups exercised on a treadmill made for animal use once daily in the dark, 6 days per week for 12 consecutive weeks. For acclimation, mice were subjected to 5 min of warm up at a 0° incline at 3 m/min, 30 min of the main exercise at 10 m/min, and 5 min of cool down at 3 m/min for the first 3 weeks. Subsequently, mice were subjected to 40 min of the main exercise at 11 m/min from weeks 4 to 6, 50 min of the main exercise at 12 m/min from weeks 7 to 9, and 50 min of the main exercise at 13 m/min from weeks 10 to 12. During treadmill running, electrical stimulation was removed to minimize stress. The exposure time to 40-Hz light flickering was the same as the exercise time.

### Preparation of tissue samples

Mice were euthanized immediately after the behavior test. To prepare brain slices, the animals were fully anesthetized with ethyl ether, perfused transcardially with 50 mM phosphate-buffered saline (PBS), and then fixed with a freshly prepared solution of 4% paraformaldehyde in 100 mM phosphate buffer (pH 7.4). The brains were then removed, post-fixed in the same fixative overnight, and transferred to a 30% sucrose solution for cryoprotection. Coronal sections with 40-μm thickness were created using a freezing microtome (Leica, Nussloch, Germany). From each group of 10 animals, 5 were used for immunohistochemistry and 5 for used for western blotting and analyses of mitochondrial function. The hippocampal for western blot analyses were immediately stored at -70 °C until use. For immunohistochemistry, two sections from each group were analyzed, resulting in a total of 10 slices.

### Behavioral analysis

### Morris water maze

The Morris water maze test was conducted to measure spatial learning and memory ability. The test animals were acclimated by swimming freely for 60 s in a pool without a platform one day before the start of training. The educational training was performed 3 times a day for 5 days with a platform. If the animal was unable to find the location of the platform within 60 s, the experimenter guided the animal to the platform. Then, the animal remained on the platform for 30 s. A probe trial was conducted 24 h after the training session; free swimming for 60 s without a platform was automatically evaluated by video tracking to determine whether the memory of the previous platform was retained or not.

### Step-through avoidance test

A step-through avoidance test was conducted to measure long-term memory. On the first day of training, the test animal was placed on a platform illuminated by a halogen light bulb, and the box door was opened. When the test animal entered the dark box, the door was closed, and the animal was allowed to stay for 20 s. This process was performed twice. In the third or final trial, the door was closed, and a foot shock at 0.2 mA current and 2 s in duration was administered once. After 24 h, the test animal was placed on a platform illuminated with a halogen light bulb. When the box door was opened, the latency to enter the dark box was measured. All times exceeding 300 s were recorded as 300 s.

### Immunohistochemistry

To visualize Aβ, neuroinflammation, and cell differentiation, immunohistochemistry was performed to detect glial fibrillary acidic protein (GFAP) and ionized calcium-binding adaptor protein-1 (Iba-1) with antigen retrieval in CA1 and the dentate gyrus (DG), doublecortin (DCX) in the DG, and Aβ in the CA1 region of the hippocampus. The sections were incubated in PBS for 10 min and then washed three times for 3 min in PBS. The sections were then incubated in 1% $H_2O_2$ for 15 to 30 min. Sections were obtained from each brain and incubated overnight with goat anti-DCX antibody (1:500; Santa Cruz Biotechnology, Dallas, TX, USA), mouse purified anti-β-amyloid antibody (1:200; Biolegend, San Diego, CA, USA), goat anti-GFAP (1;500; Abcam, Cambridge, UK), and rabbit Iba-1 (1:500; Abcam), followed by incubation with biotinylated goat, mouse, rabbit secondary antibody (1:200; Vector Laboratories, Burlingame, VT, USA) for another 90 min. The secondary antibody was amplified using the Vector Elite ABC Kit (1:100; Vector Laboratories). Antibody-biotin-avidin-peroxidase complexes were visualized using the 3,3, Diaminobenzidine (DAB) Substrate Kit (Vector Laboratories). The slides were air-dried overnight at room temperature, and the coverslips were mounted using Permount.

### Immunofluorescence

NeuN/BrdU-positive cells in the DG were evaluated by immunofluorescence. In brief, the brain sections were permeabilized by incubation in 0.5% Triton X-100 in PBS for 20 min, incubated in 50% formamide-2 × standard saline citrate at 65 °C for 2 h, denatured in 2 N HCl at 37 °C for 30 min, and then rinsed twice in 100 mM sodium borate (pH 8.5). The sections were incubated overnight with rat anti-BrdU antibody (1:200; Abcam) and mouse anti-NeuN antibody (1:200; Millipore, Temecula, CA, USA). The brain sections were then washed in PBS and incubated with appropriate secondary antibodies for 1 h. The secondary antibodies were anti-mouse IgG Alexa Fluor-488 and anti-rat IgG Alexa Fluor-560. Images were captured using an FV3000 confocal microscope for a subsequent Z-section (1 μm) analysis (Olympus, Tokyo, Japan).

### TUNEL staining

To visualize DNA fragmentation, TUNEL staining was performed using an In Situ Cell Death Detection Kit (Roche Diagnostics, Risch-Rotkreuz, Switzerland) according to the manufacturer's protocol. Sections were post-fixed in ethanol-acetic acid (2:1), rinsed, incubated with proteinase K (100 mg/mL), and then rinsed again. Next, they were incubated in 3% $H_2O_2$, permeabilized with 0.5% Triton X-100, rinsed, and incubated in the TUNEL reaction mixture. The sections were rinsed and visualized using Converter-POD with 0.03% DAB, counterstained with Cresyl violet, and mounted onto gelatin-coated slides. The slides were air-dried overnight at room temperature. A cover slip was added using Permount mounting medium.

### Western blotting

Hippocampal tissues were homogenized on ice and lysed in lysis buffer containing 50 mM Tris–HCl (pH 7.5), 150 mM NaCl, 0.5% deoxycholic acid, 1% Nonidet P40, 0.1% sodium dodecyl sulfate, 1 mM PMSF, and leupeptin 100 mg/mL. The protein content was measured using a Colorimetric Protein Assay Kit (Bio-

Rad, Hercules, CA, USA). Thirty micrograms of protein were separated on sodium dodecyl sulfate-polyacrylamide gels and transferred onto a nitrocellulose membrane, which was incubated with mouse β-actin (1:1000; Santa Cruz Biotechnology), GAPDH (1:3000; Santa Cruz Biotechnology), t-Akt and p-Akt (1:1000; Cell Signaling, Danvers, MA, USA), t-GSK3β and p-GSK3β (ser 9) (1:1000; Cell Signaling), t-Tau and p-Tau (ser202/Thr205, 1:1000; Thermo Fisher, Waltham, MA, USA), amyloid precursor protein (APP; 1:1000; Abcam), adenine nucleotide translocator (ANT1/2, 1:1000, Proteintech, Rosemont, IL, USA), voltage-dependent anion-selective channel protein (VDAC1, 1:1000: Bioss, Woburn, MA, USA), cyclophilin D (Cyp-D, 1:1000; Thermo Fisher), tumor necrosis factor-α (TNF-α, 1:1000; Abcam), interleukin-6 (IL-6, 1:700; Abcam), Bcl-2 and cytochrome C (1:1000; Santa Cruz Biotechnology), Bax (1:1000; Cell Signaling), cleaved caspase-3 (1:700; Cell Signaling), brain-derived neurotrophic factor (BDNF; 1:1000; Alomone, Jerusalem, Israel), postsynaptic density protein 95 (PSD95, 1:1000; Cell Signaling), synaptophysin (1:1000; Abcam), β-actin and GAPDH (1:3000; Santa Cruz Biotechnology), and COX IV (1:1000, Cell Signaling) primary antibodies. Horseradish peroxidase-conjugated secondary anti-mouse antibodies were used for Bcl-2, p-Tau, cytochrome C, β-actin, and GAPDH; anti-rabbit conjugated secondary antibodies were used for t-Akt, p-Akt, t-tau, p-tau, t-GSK3β, APP, ANT1/2, VDAC1, Cyp-D, Bax, cleaved caspase-3, BDNF, PSD95, synaptophysin, and COX IV.

### Isolation of hippocampal mitochondria

Mitochondria were isolated from the mouse brain using a Mitochondria Isolation Kit for Tissue (Thermo #89801; Thermo Fisher Scientific) according to the manufacturer's instructions. Briefly, homogeneous suspensions of hippocampal tissue were prepared using a pre-chilled homogenizer (T 10 Basic Ultra-Turrax; Ika, Staufen im Breisgau, Germany). The hippocampal suspensions were spun at 1,000 × *g* for 5 min at 4 °C. The pellet was suspended in 800 µL of bovine serum albumin/reagent A solution and incubated for 2 min before adding 10 µL of isolation reagent B. After incubation for 5 min with intermittent vortexing, 800 µL of reagent C was added. The resulting cell lysate was centrifuged at 700 × *g* for 10 min at 4 °C, after which the supernatant was transferred to a new tube and spun at 3,000 × *g* for 15 min at 4 °C. The supernatant (cytosolic fraction) was collected for analysis. After washing with mitochondrial isolation reagent C, the mitochondrial pellet was lysed with 2% CHAPS in Tris-buffered saline containing protease inhibitors. The samples were stored at -80 °C until use.

### Mitochondrial $Ca^{2+}$ retention capacity

The mitochondrial calcium retention capacity was tested to assess the susceptibility of the permeability transition pore (PTP) to opening. Briefly, after grinding the hippocampal tissue, overlaid traces of changes in fluorescence induced by Calcium Green-5 N were measured continuously (ΔF/min) at 37 °C during state 4 respiration using a Spex FluoroMax 4 spectrofluorometer (Horiba Scientific, Edison, NJ, USA). After establishing the background ΔF (hippocampal tissue in the presence of 1 µM Calcium Green-5 N, 1 U/mL hexokinase, 0.04 mM EGTA, 1.5 nM thapsigargin, 5 mM 2-deoxyglucose, 5 mM glutamate, 5 mM succinate, and 2 mM malate), the reaction was initiated by $Ca^{2+}$ pulses (12.5 nM), with excitation and

emission wavelengths set to 506 nm and 532 nm, respectively. The total mitochondrial $Ca^{2+}$ retention capacity prior to PTP opening (i.e., release of $Ca^{2+}$) is expressed in units of pmol/mg.

### Mitochondrial Ho Emission

$H_2O_2$ emission was measured at 37 °C (ΔF/min) during state 4 respiration (10 μg/mL oligomycin) by continuously monitoring the oxidation of Amplex Red (excitation/emission λ = 563/587 nm) using a Spex FluoroMax 4 spectrofluorometer with 10 μM Amplex Red, 1 U/mL horseradish peroxidase, 10 μg/mL oligomycin, 1 mM malate + 2 mM glutamate (complex I substrates), 3 mM succinate (complex II substrate), and 10 mM glycerol-3-phosphate (lipid substrate). The $H_2O_2$ emission rate after subtracting the background value from the standard values (standard curve) was calculated from the ΔF/min gradient values and results are expressed in units of pmol/min/mg tissue weight.

### Statistical analyses

Cell counting and optical density quantification were performed using Image-Pro Plus (Media Cyberbetics Inc., Rockville, MD, USA) attached to a light microscope (Olympus). The data were analyzed using one-way analysis of variance, followed by Tukey post-hoc tests. All values are expressed as means ± standard error of the mean, and p values < 0.05 were considered significant.

# Results

### Effect of exercise and 40-Hz light flicker on spatial working learning, memory, and long-term memory in the early 3xTg-AD

As summarized in Fig. 1, Morris water maze and step-through avoidance tests were performed to evaluate spatial learning, memory, and long-term memory. Spatial learning was evaluated as the time until the animal visited the platform. In all groups except the AD group ($p < 0.001$), the time to find the platform was shorter shortened from day 3, and there were no differences among treatment groups. With respect to the spatial learning ability, the time to find the platform for each group was as follows: Day 3; CON group ($p = 0.022$), AD + 40 ($p = 0.008$), AD + EX ($p = 0.001$), AD + 40 + EX ($p < 0.001$), Day 4; CON group ($p = 0.001$), AD + 40 ($p = 0.008$), AD + EX ($p = 0.001$), AD + 40 + EX ($p < 0.001$), Day 5 ($p < 0.001$). For the spatial memory test at 24 h after 5 days of training, spatial memory was lower in the AD group than in the CON group ($p < 0.001$) and increased in the 40-Hz light flicker group ($p < 0.001$), exercise group ($p < 0.001$), and combination treatment group ($p < 0.001$). The effect of the combination of the two treatments on spatial memory was greater than that of single treatments ($p < 0.001$) and spatial memory in the combined treatment group was equal to or better than that in the non-transgenic CON group ($p = 0.049$). Even long-term memory, as evaluated by the step-through avoidance test, was lower ($p < 0.001$) in the AD group and higher in the 40-Hz light flicker group ($p = 0.001$), exercise group ($p = 0.001$), and combination treatment group ($p < 0.001$) than in the CON group. The combination treatment showed better results than those for the single treatment groups, i.e., the 40-Hz light flicker group ($p = 0.004$) and exercise group ($p = 0.005$), with an increment to the level observed in the non-transgenic CON group.

### Effect of exercise exposure with 40-Hz light flicker on Akt, GSK3β, APP, tau, and Aβ in the hippocampus in early 3xTg-AD

In the hippocampus, Akt, GSK3β, Tau, and APP protein expression changes were analyzed by western blotting (Fig. 2). For comparison among groups, the value for the CON group was set to 1.0 and relative values for each treatment group were compared. Compared with the CON group, the t-Akt/p-Akt ($p < 0.001$) and p-GSK3β/GSK3β ratios ($p < 0.001$) were lower and the t-Tau/p-Tau ratio ($p < 0.001$) and APP protein ($p < 0.001$) expression level were higher in the AD group. Akt and GSK3β levels were increased in 40-Hz light flicker group (t-Akt/p-Akt ratio: $p = 0.037$; p-GSK3β/GSK3β ratio: $p = 0.033$), exercise group (t-Akt/p-Akt ratio: $p = 0.034$; p-GSK3β/GSK3β ratio: $p = 0.008$), and the combination treatment group (t-Akt/p-Akt ratio: $p < 0.001$; p-GSK3β/GSK3β ratio: $p < 0.001$), and the combination treatment had a greater effect than that of single treatment with 40-Hz light flicker (t-Akt/p-Akt ratio: $p = 0.022$; p-GSK3β/GSK3β ratio: $p = 0.007$) or exercise (t-Akt/p-Akt ratio: $p = 0.024$; p-GSK3β/GSK3β ratio: $p = 0.029$). Tau and APP levels were decreased in the 40-Hz light flicker group (t-tau/p-tau ratio, APP, $p < 0.001$, respectively) and exercise group (t-tau/p-tau ratio, APP, $p < 0.001$, respectively) and in the combination treatment group (t-tau/p-tau ratio, APP $p < 0.001$, respectively).

The combination treatment showed better results than those for the single treatment with 40-Hz light flicker (t-tau/p-tau ratio, each APP $p < 0.001$) or exercise (t-tau/p-tau ratio, APP each $p < 0.001$). To identify Aβ-positive cells, CA1 of the hippocampus was analyzed by immunohistochemistry. In the CON group, Aβ-positive cells were not found in CA1 of the hippocampus. Compared with the AD group, hippocampal CA1 Aβ-positive cells ($p < 0.001$) were decreased in the 40-Hz light flicker group, exercise group, and combination treatment group, and the effects for the combination treatment were greater than those for the single treatment of 40-Hz light flicker ($p = 0.001$) and exercise ($p < 0.001$). In particular, Akt/GSK3β/tau/APP protein expression levels improved to the level observed in the non-transgenic CON group.

### Effect of exercise exposure with 40-Hz light flicker on neuroinflammation and pro-inflammatory cytokines in the hippocampus in early 3xTg-AD

To evaluate neuroinflammation in the hippocampus, GFAP-positive astrocytes and Iba-1-positive microglial cells were analyzed by immunohistochemistry (Fig. 3). Compared with the CON group, neuroinflammation was increased in the hippocampal CA1 and DG in the AD group (GFAP and Iba-1: $p < 0.001$). Compared with the AD group, GFAP and Iba-1 levels were lower in the 40-Hz light flicker group, exercise group, and combination treatment group (GFAP ($p = 0.002$) and Iba-1 ($p = 0.001$) from CA1, and GFAP ($p < 0.001$) and Iba-1 ($p < 0.001$) from DG). Additionally, the combined treatment with 40-Hz light flicker and exercise decreased these markers in the CA1 and DG of the hippocampus more substantially than the decreases in response to single treatments (GFAP and Iba-1: $p < 0.001$). Levels of pro-inflammatory cytokines in the hippocampus, i.e., TNF-α and IL-6, were analyzed by western blotting. Levels in the CON group were set to 1.0 and used to determine relative values in each group. The expression levels of pro-inflammatory cytokines were higher in the AD group than in the CON group (TNF-

α: $p < 0.001$; IL-6: $p < 0.001$). These levels were lower in the 40-Hz light flicker group (TNF-α: $p = 0.003$; IL-6: $p = 0.004$), exercise group (TNF-α: $p = 0.008$; IL-6: $p < 0.001$), and combination treatment group (TNF-α, IL-6: each $p < 0.001$) than in the AD groups. Additionally, the combination treatment of 40-Hz light flicker and exercise resulted in greater decreases than either single treatment (40-Hz light flicker: TNF-α: $p = 0.004$, IL-6: $p < 0.001$; exercise: TNF-α, IL-6: both $p = 0.001$). Neuroinflammation and pro-inflammatory cytokine expression recovered to the levels in the non-transgenic CON group.

### Effect of exercise exposure with 40-Hz light flicker on mitochondrial function and PTP (mPTP) opening in the hippocampus of early 3xTg-AD

To determine mitochondrial function and PTP in the hippocampus, mitochondrial $Ca^{2+}$ retention capacity, $H_2O_2$ emission, and levels of ANT1/2, VDAC1, and Cyp-D were evaluated (Fig. 4). In the hippocampus, the mitochondrial $Ca^{2+}$ retention capacity was lower in the AD group than in the CON group ($p < 0.001$). It was higher in the 40-Hz light flicker group ($p = 0.015$), exercise group ($p = 0.006$), and combined treatment group ($p < 0.001$) than in the AD group. In addition, the increase in the $Ca^{2+}$ retention capacity was greater for the combined treatment than for single treatments (40-Hz light flicker: $p = 0.006$; exercise: $p = 0.015$). To determine the mPTP opening sensitivity, the CON group of $Ca^{2+}$ retention in the CON group (set to 100%) was used as the baseline. Compared with the CON group, the mPTP opening sensitivity was lower in the AD group ($p < 0.001$) and higher in 40-Hz light flicker ($p = 0.040$), exercise ($p = 0.036$), and combined treatment groups ($p < 0.001$). Additionally, the increase in sensitivity was greater for the combination treatment than for single treatments (40-Hz light flicker: $p = 0.041$; exercise: $p = 0.045$). Furthermore, mPTP-related membrane proteins were analyzed in isolated mitochondria. Mitochondrial membrane proteins, including ANT1/2, VDAC1, and Cyp-D, were more highly expressed in the AD group than in the CON group (all $p < 0.001$). Expression was suppressed in the 40-Hz light flicker group (ANT1/2: $p < 0.001$, VDAC1: $p = 0.001$, Cyp-D: $p = 0.001$), exercise group (all $p < 0.001$), and combination treatment group (all $p < 0.001$). Protein levels were lower for the combination treatment than for single treatments (40-Hz light flicker (ANT1/2: $p = 0.006$, VDAC1: $p = 0.002$, Cyp-D: $p = 0.003$; Exercise (ANT1/2: $p = 0.031$, VDAC1: $p = 0.034$, Cyp-D: $p = 0.014$). The mitochondrial $H_2O_2$ emission rate was calculated on Complex I substrate (glutamate + malate; GM), Complex 2 substrate (succinate; GMS), and a lipid substrate (glycerol-3 phosphate; GMSG3P). For the $H_2O_2$ emission rate, an ROS marker, there were no differences among groups on the Complex 1 substrate. On the Complex 2 substrate, compared to the CON group, the $H_2O_2$ emission rate was higher in the AD group ($p = 0.001$) and was significantly lower in the combination treatment group ($p = 0.005$) but not in other treatment groups. Finally, for the lipid substrate, the $H_2O_2$ emission rate was also higher in the AD group than in the CON group ($p < 0.001$). The emission rate decreased in the 40-Hz light flicker group ($p = 0.001$), exercise group ($p = 0.007$), and combination treatment group ($p < 0.001$). The reduction in the emission rate was greater for the combination treatment than for each treatment group (40-Hz light flicker: $p = 0.031$, exercise: $p = 0.003$). The combination treatment was more effective in improving mitochondrial function and permeability of the hippocampus, with recovery to the levels observed in the non-transgenic CON group.

### Effect of exercise exposure with 40-Hz light flicker on apoptosis and cell death in the hippocampus in early 3xTg-AD

Changes in apoptosis-related proteins in the hippocampus, including Bax, Bcl-2, cytochrome c, and cleaved caspase-3, were analyzed, and TUNEL-positive cells were analyzed to determine cell death (Fig. 5). Values in the CON group value were set to 1.0 and used to obtain relative values for comparisons among groups. Compared with the CON group, Bax, cytochrome c, and cleaved caspase-3 levels were higher and Bcl-2 levels were lower in the AD group (all $p < 0.001$). The expression levels of Bax, cytochrome c, and cleaved caspase-3 decreased in the individual treatment groups [40-Hz light flicker group (Bax: $p < 0.001$, cytochrome c: $p = 0.002$, caspase-3: $p < 0.001$), exercise group (Bax: $p < 0.001$, cytochrome c: $p = 0.007$, caspase-3: $p < 0.001$)] and combined treatment group (all $p < 0.001$)], and Bcl-2 levels increased in the 40-Hz light flicker group ($p = 0.042$), exercise group ($p = 0.039$), and combined treatment group ($p < 0.001$). Additionally, the decrease in apoptosis was greater in the combination treatment group than in each single treatment group (40-Hz light flicker: Bax: $p = 0.028$, Bcl-2: $p = 0.001$, cytochrome c: $p = 0.042$, caspase-3: $p = 0.002$; exercise: 40-Hz light flicker: Bax: $p = 0.027$, Bcl-2: $p = 0.002$, cytochrome c: $p = 0.016$, caspase-3: $p = 0.044$). TUNEL-positive cells were analyzed to determine final cell death rates in the hippocampus. In the hippocampus, the number of TUNEL-positive cells was higher in the AD group ($p < 0.001$) and lower in the 40-Hz light flicker group ($p < 0.001$), exercise group ($p = 0.002$), and combined treatment group ($p < 0.001$) than in the CON group. Additionally, cell death was greater in the combination treatment group than in the single treatment groups (all $p < 0.001$). Therefore, simultaneous treatment was more effective in inhibiting hippocampal apoptosis and cell death, with recovery to levels observed in the non-transgenic CON group.

### Effect of exercise exposure with 40-Hz light flicker on BDNF, synaptophysin, and PSD95 in the hippocampus in early 3xTg-AD

The expression levels of the synaptic proteins BDNF, PSD 95, and synaptophysin were investigated in the hippocampus (Fig. 6). Levels in the CON group were set to 1.0 to obtain relative values in each group. Compared with the CON group, protein expression levels were decreased in the AD group (all $p < 0.001$) but were higher in each treatment group, including the 40-Hz light flicker group (BDNF: $p = 0.032$, synaptophysin: $p = 0.005$, PSD95: $p = 0.046$), exercise group (BDNF: $p = 0.015$, synaptophysin: $p = 0.001$, PSD95: $p < 0.001$), and combination treatment group (all $p < 0.001$). The increases in expression were higher in the combination treatment group than in single treatment groups (40-Hz light flicker: all $p < 0.001$, exercise: BDNF and synaptophysin: $p < 0.001$, PSD95: $p = 0.001$). Accordingly, the combined treatment was more effective in increasing the expression of synapse-related proteins; in particular, BDNF levels were equal to or better than those in the non-transgenic CON group.

### Effect of exercise exposure with 40-Hz light flicker on cell differentiation and neurogenesis in the hippocampal DG of early 3xTg-AD

DCX-positive cells and NeuN/BrdU-positive cells were evaluated to investigate cell differentiation and neurogenesis in the hippocampus (Fig. 7). The frequencies of hippocampal DCX-positive cells and

NeuN/BrdU-positive cells were lower in the AD group than in the CON group (both $p < 0.001$) but were increased in the 40-Hz light flicker group (DCX: $p < 0.001$, NeuN/BrdU: $p = 0.004$), exercise group, and combination treatment group (both $p < 0.001$). The increases in DCX-positive cells ($p < 0.001$) and NeuN/BrdU-positive cells (40-Hz light flicker: $p < 0.001$, exercise: $p = 0.001$) were greater with the combined treatment than with single treatments. Therefore, the combination of the two treatments increased cell differentiation and neurogenesis in the hippocampus, with recovery to the levels observed in the non-transgenic CON group.

# Discussion

AD, the primary cause of dementia, begins in the temporal lobe and encroaches on all areas of the brain. Memory impairment is a major symptom because the hippocampus, the central organ involved in memory, is located in the temporal lobe. Similar to many diseases, treatment at the initial stage of AD is crucial. Various studies have shown that 3xTg-AD mice begin to develop deficits in short-term and long-term meomory, spatial learning and memory at 4 months [22], 6 months, and 6.5 months of age [23, 24]. Although these findings provide insight into the starting point of various cognitive deficits, they develop continuously over time [23]. Consistent with previous studies, we detected the impairment of spatial learning, memory, and long-term memory in the AD group. These AD-related cognitive dysfunctions support the amyloid cascade hypothesis, in which disease onset is characterized by changes in Aβ, followed by a series of events, including the accumulation of toxic forms of tau, which induces apoptosis [1]. Amyloid plaque deposition begins in the neocortex several years before the onset of symptoms and gradually spreads to the hippocampus, diencephalon, striatum, brainstem, and finally the cerebellum [25]. In both the human brain and animal models, the expression of APP, presenilin mutations, and plaques, which are related to AD, are not only associated with synaptic loss but also with a deficiency of memory and synaptic plasticity [26–29]. Pathological forms of Aβ and tau as well as glia-mediated neuroinflammation play roles in synatptotoxicity [30].

Microglial cells and astrocytes exhibit changes in gene expression, morphology, and secretion in response to toxic stimuli in the brain, and these alterations affect other cells, including neurons [1]. The activation of microglial cells and astrocytes in the early stage of AD results in microgliosis, astrogliosis, impairments in amyloid and tau removal, neurotoxin release, and pro-inflammatory cytokine release [31–35]. Previous studies have reported that the frequencies of GFAP-positive astrocytes and Iba-1 microglial cells are increased in the 3xTg-AD hippocampus at 6 and 10 months [36–38]. Microglial cells and astrocytes associated with amyloids secrete pro-inflammatory cytokines, such as IL-1β, IL-6, and TNF-α [39]. In various animal models of AD, the entire brain, including the hippocampus and hypothalamus, shows increases in IL-6 and TNF-α at the mRNA and protein levels [40–42]. In particular, IL-6 results in the release of a cascade of pro-inflammatory cytokines by microglia and astrocytes [43]. Consistent with previous results, in this study, tau hyperphosphorylation and APP expression were higher, p-Akt and p-GSK3β in the hippocampus were lower, and Aβ-positive cells in CA1 were higher in the AD group than in the control group. These results suggested that the dysregulation of Tau and Aβ increased the expression of TNF-α and IL-6 by activating astrocyte and microglia in the hippocampus. As such, Aβ and tau and

phosphorylation are associated with increases in pro-inflammatory cytokine levels via the activation of microglia and astrocytes and contribute to $Ca^{2+}$ dysregulation [44], ROS [39], and cell death [45]. Mitochondria provide an important buffer to regulate the calcium concentration during signaling, which is particularly important for excitatory cells, such as neurons [46].

Mitochondrial dysfunction related to Aβ, such as ROS release [47, 48] and the disruption of calcium homeostasis [49], is frequently observed in patients with AD and in animal models. The mPTP is associated with Aβ-induced mitochondrial dysfunction, such as a disturbance of intracellular calcium regulation, ROS generation, and the release of pro-apoptotic factors [50]. In previous studies, mitochondria from mice with AD had much lower calcium capacities than those of non-transgenic mouse mitochondria, and the impaired $Ca^{2+}$ uptake capacity, starting from 6 months, decreased gradually. This decreased $Ca^{2+}$ retention capacity increased the expression of cyclophilin D (cyp-D), a mitochondrial matrix component, and mPTP components, such as voltage-dependent anion channel 1 (VDAC1) of the outer membrane [51, 52]. Adenine nucleotide translocator (ANT), a component of the inner membrane, binds to cyp-D, and cyp-D and ANT interact with Aβ. ANT strongly interacts with Aβ to change mPTP regulation and is related to mitochondrial dysfunction [53]. Additionally, $H_2O_2$ is an important ROS that induces oxidative damage, and an increase in mitochondrial $H_2O_2$ is significantly associated with the onset of AD [51, 54]. Mitochondrial dysfunction, including increases in mPTP and ROS, can induce increased apoptosis. Increased levels of Cyp-D, VDAC1, and ANT increase apoptosis [51–53], and $H_2O_2$ penetrates all tissue compartments, triggers oxidative toxicity, and induces apoptosis [55]. Mitochondria play an important role in the regulation of fundamental processes of neuroplasticity [56], and alterations in mitochondrial function are associated with changes in synaptic plasticity [57].

Mitochondrial dysfunction caused by Aβ may be related to neuroplasticity changes. Synapse-related proteins, such as BDNF, PSD95, and synaptophysin, in the hippocampus in the early stage, DCX, and neurogenesis are decreased in various AD animal models [58–62]. In this study, the $Ca^{2+}$ retention capacity was lower and $H_2O_2$ emission was higher in hippocampal mitochondria in the AD group than in the control group, and mPTP-related proteins were overexpressed, indicating a decline in mitochondrial function. Furthermore, cell death increased, as determined by increases in Bax, a pro-apoptotic factor, cytochrome c, and cleaved caspase-3 and decreases in Bcl-2, an anti-apoptotic factor. Additionally, synapse-related proteins, such as BDNF, PSD95, and synaptophysin, as well as DCX and neurogenesis decreased. In patients with AD, decreased levels of BDNF in the blood and brain and impaired neurogenesis have been observed in the early stages of the disease with decreased cognitive function [63–65]. There is a positive correlation between the BDNF concentration and cognitive function [66]. As such, it is believed that Aβ production or aggregation and tau phosphorylation, via direct or indirect pathways, affect neuroinflammation, mitochondrial function, apoptosis, and synapses in various brain regions, including the hippocampus, leading to cognitive decline.

Altered gamma oscillations have been observed in several brain regions in various neurological and mental disorders, including a decrease of spontaneous gamma synchronization in patients with AD and a

decrease in gamma power in several AD mouse models [67–70]. Although gamma oscillations could not be measured in this study, they are associated with functional decline in AD, as established in an APP/PS1 model of AD [71]. Gamma oscillations in the hippocampus are degraded according to the concentration and time of Aβ [72], and damaged mitochondrial function abolishes gamma oscillations in the hippocampal network [73]. In a transgenic mouse model of AD, theta-gamma coupling was found to be defective in the subiculum, the major output area of the hippocampus [74]. Recent work has shown that 40-Hz light flicker stimulation, a non-invasive treatment method, reduces Aβ and phosphorylated tau in various AD animal models by entraining gamma oscillations through the visual cortex. This improves spatial learning and memory by reducing the progression of the degenerative state of neurons, improving synaptic function, enhancing neuronal protective factors, reducing DNA damage, and reducing the inflammatory response of microglia [19, 20, 75].

Furthermore, 40-Hz auditory stimulation boosts hippocampal function by gamma entrainment, and combined visual and auditory stimulation improves cognitive function by reducing amyloid pathology [21]. In this study, Aβ and phosphorylated tau in the hippocampus were attenuated in the 40-Hz light flicker group, as were Iba-1-positive microglial cells and GFAP-positive astrocytes. Long-term 40-Hz light flicker stimulation through the visual cortex stabilized gamma oscillations and alleviated Aβ, tau, and inflammatory responses in the hippocampus.

In the hippocampus, the mitochondrial $Ca^{2+}$ retention capacity and alleviated $H_2O_2$ emissions may have improved cognitive function via the inhibition of apoptosis, increased neurogenesis, and improved neuroplasticity, including increased synaptic protein expression. Exercise, another non-invasive intervention, has a positive effect on brain function and is a candidate lifestyle intervention for reducing the incidence of dementia and AD [76]. Physical exercise decreases Aβ and tau levels and increases memory, and high-quality exercise is associated with decreased Aβ in the plasma and brain of patients with AD [77–79]. Additionally, exercise is considered a powerful tool to prevent neuroinflammation and prevent the decline of cognitive function [80].

Liu et al. [81] showed that exercise increases the expression of Akt/GSK3β pathway members in the 3xTg-AD model, decreases Aβ deposition, and decreases Iba-1-positive microglial cells and GFAP-positive astrocytes in the hippocampal DG. Exercise at the early stage of AD has a protective effect on cognitive function by reducing Aβ plaques and GFAP-positive astrocytes in the hippocampus and increasing neurogenesis [82]. Exercise with anti-inflammatory effects inhibits pro-inflammatory cytokines, such as TNF-α, IL-6, and IL1β, in the tau-transgenic hippocampus [83].

In this study, the AD exercise group showed increases in Akt/GSK3β pathway expression, decreases in tau and Aβ, and decreases in excessive Iba-1-positive microglial cells and GFAP-positive astrocytes, as well as decreases in TNF-α and IL-6 expression in the hippocampus. Exercise induces an antioxidant defense system, which reduces ROS levels, and adaptation to long-term regular exercise directly decreases ROS production, reduces oxidative damage [80], and may improve mitochondrial function. In brain regions, including the hippocampus, cortex, and cerebellum, increased mitochondrial $Ca^{2+}$ accumulation and

calcium-induced mPTP opening by exercise increased resistance to exercise and reduced apoptosis, suggesting that exercise has a protective effect against mitochondrial degeneration and cell death [84, 85]. Furthermore, exercise inhibits the overexpression of various membrane-related proteins, such as ANT1/2, cyp-D, and VDAC1, and $H_2O_2$, an ROS marker [85]. Therefore, in an AD transgenic and systemic model, Bax, cytochrome c, caspase 3, and caspase 9 levels are decreased and Bcl-2 levels are increased after exercise [86, 87]. Brain mitochondrial function increases in a BDNF concentration-dependent manner [88], and BDNF expression increases in response to exercise [89, 90]. Neurotrophin is associated with learning, memory, neuronal activity, and plastic responses [91, 92]. Decreases in synapse-related proteins, such as PSD95 and synaptophysin, in the hippocampus in the early stage of AD are also increased by exercise [93, 94]. Exercise, especially through increased neurogenesis with decreased Aβ in the AD hippocampus and increased BDNF, improves cognitive function [95].

In the exercise group in this study, mitochondrial function improved with an increased $Ca^{2+}$ retention capacity, decreased mPTP proteins, including ANT1/2, VDAC1, and cyp-D, decreased $H_2O_2$ emissions in the hippocampal mitochondria, and reduced cell death via decreased Bax, cytochrome c, and caspase-3 and increased Bcl-2. Additionally, BDNF, synaptophysin, PSD95, and neurogenesis were increased. In early AD, exercise seems to have a protective effect on cognitive function by improving the neuroplasticity of the mitochondria and hippocampus.

Under specific environmental conditions, such as 40-Hz light flicker, a non-invasive method, exercise seemed to have a greater effect. A limitation of this study was the inability to analyze gamma oscillations. However, under an environment where gamma oscillations are entrained through 40-Hz light flicker by the visual cortex and improve Aβ and tau pathology by inducing a variety of positive cellular changes, exercise may result in the stimulation of various brain regions via various myokines secreted from the muscles.

# Conclusion

In this study, the combination of 40-Hz light flicker and exercise, both of which are non-pharmacological and non-invasive methods, improved mitochondrial function and neuroplasticity by repairing Aβ and tau, which are closely linked to AD. The method may be effective for preventing cognitive decline by suppressing the expression of Aβ and tau, neuroinflammation, and mitochondrial function and by protecting against deficits in neuroplasticity of the hippocampus in the early stage of AD. Future studies focused on a wider range of parameters and clinical applications are needed.

# Abbreviations

3xTg-AD: Triple transgenic mouse model of Alzheimer’s disease; AD: Alzheimer’s disease; Aβ: Amyloid-β; GFAP: Glial fibrillary acidic protein; Iba-1: ionized calcium-binding protein 1; BDNF: Brain-derived neurotrophic factor; ANT: Adenine nucleotide translocator; VDAC: voltage-dependent anion channel; Cyp-D: cyclophilin D; mPTP: mitochondrial permeability transition pore; BrdU: 5-bromo-2'-deoxyuridine; DG:

Dentate gyrus; GSK3β: Glycogen synthase 3 beta; PSD95: Postsynaptic density protein 95; ROS: Reactive oxygen species; TUNEL: Terminal deoxynucleotidyl transferase dUTP nick end labeling

# Declarations

### Ethics approval and consent to participate

All animal experiments were performed in accordance with the guidelines of the National Institutes of Health and the Korean Academy of Medical Science. The study protocol was approved by the KyungHee University Institutional Animal Care and Use Committee (approval number KHUASP [SE]-17-103).

### Consent for publication

Not applicable

### Competing interests

The authors declare that they have no competing interests.


### Funding

This work was supported by the Ministry of Education of the Republic of Korea and the National Research Foundation of Korea (NRF-2017S1A5B5A02025250).


### Authors' contributions

S-S P and H-S P performed data acquisition, data analysis, writing of original draft and project administration resources. C-J K and S-S B performed supervision, review and editing. T-W K performed conceptualization, data acquisition, funding acquisition, project administration resources, supervision, writing, review, and editing. All authors read and approved the final manuscript.

# References


1. Henstridge CM, Hyman BT, Spires-Jones LT. Beyond the neuron–cellular interactions early in Alzheimerdisease pathogenesis. Nat Rev Neurosci. 2019;20:94-108.
2. Hardy JA, Higgins GA. Alzheimer's disease: the amyloid cascade hypothesis. Science. 1992;256: 184–185.
3. Karran E, De Strooper B. The amyloid cascade hypothesis: are we poised for success or failure? J. Neurochem. 2016;139:237–252.
4. Takahashi RH, Capetillo-Zarate E, Lin MT, Milner TA, Gouras GK. Co-occurrence of Alzheimer's disease ß-amyloid and pathologies at synapses. Neurobiol Aging. 2010;31:1145-1152.
5. Colom-Cadena M, Spires-Jones T, Zetterberg H, Blennow K, Caggiano A, Dekosky ST, et al. The clinical promise of biomarkers of synapse damage or loss in Alzheimer's disease. Alzheimers Res

Ther. 2020;12(1):21.

6. Heneka MT, O'Banion MK, Terwel D, Kummer MP. Neuroinflammatory processes in Alzheimer's disease. J Neural Transm (Vienna). 2010;117:919-947.
7. Zhao J, O'Connor T, Vassar R. The contribution of activated astrocytes to Aβ production: implications for Alzheimer's disease pathogenesis. J Neuroinflammation. 2011;8:150.
8. McGeer PL, McGeer EG. The inflammatory response system of brain: implications for therapy of Alzheimer and other neurodegenerative diseases. Brain Res Brain Res Rev. 1995;21:195-218.
9. Hoekstra JG, Hipp MJ, Montine TJ, Kennedy SR. Mitochondrial DNA mutations increase in early stage Alzheimer disease and are inconsistent with oxidative damage. Ann Neurol. 2016;80:301-306.
10. Hauptmann S, Scherping I, Dröse S, et al. Mitochondrial dysfunction: an early event in Alzheimer pathology accumulates with age in AD transgenic mice. Neurobiol Aging. 2009;30:1574-1586.
11. Reddy PH. Amyloid beta, mitochondrial structural and functional dynamics in Alzheimer's disease. Exp Neurol. 2009;218:286-292.
12. Swerdlow RH, Khan SM. The Alzheimer's disease mitochondrial cascade hypothesis: an update. Exp Neurol. 2009;218:308-315.
13. Aliev G, Palacios HH, Walrafen B, Lipsitt AE, Obrenovich ME, Morales L. Brain mitochondria as a primary target in the development of treatment strategies for Alzheimer disease. Int J Biochem Cell Biol. 2009;41:1989-2004.
14. Mancuso M, Coppedè F, Murri L, Siciliano G. Mitochondrial cascade hypothesis of Alzheimer's disease: myth or reality?. Antioxid Redox Signal. 2007;9:1631-1646.
15. Swerdlow RH, Khan SM. A "mitochondrial cascade hypothesis" for sporadic Alzheimer's disease. Med Hypotheses. 2004;63:8-20.
16. Geda YE, Roberts RO, Knopman DS, Christianson TJH, Pankratz VS, Ivnik RJ, et al. Physical exercise, aging, and mild cognitive impairment: a population-based study. Arch Neurol. 2010;67:80-86.
17. Radak Z, Hart N, Sarga L, Koltai E, Atalay M, Ohno H, et al. Exercise plays a preventive role against Alzheimer's disease. J Alzheimers Dis. 2010;20:777-783.
18. Hawley JA, Hargreaves M, Joyner MJ, Zierath JR. Integrative biology of exercise. Cell. 2014;159:738-749.
19. Iaccarino HF, Singer AC, Martorell AJ, Rudenko A, Gao F, Gillingham T, et al. Gamma frequency entrainment attenuates amyloid load and modifies microglia. Nature. 2016;540:230-235.
20. Singer AC, Martorell AJ, Douglas JM, Abdurrob F, Attokaren MK, Tipton J, et al. Noninvasive 40-Hz light flicker to recruit microglia and reduce amyloid beta load. Nat Protoc. 2018;13:1850-1868.
21. Martorell AJ, Paulson AL, Suk HJ, Abdurrob F, Drummond GT, Guan W, et al. Multi-sensory Gamma Stimulation Ameliorates Alzheimer's-Associated Pathology and Improves Cognition. Cell. 2019;177:256-271.
22. Billings LM, Oddo S, Green KN, McGaugh JL, LaFerla FM. Intraneuronal Abeta causes the onset of early Alzheimer's disease-related cognitive deficits in transgenic mice. Neuron. 2005;45:675-688.

23. Clinton LK, Billings LM, Green KN, Caccamo A, Ngo J, Oddo S, et al. Age-dependent sexual dimorphism in cognition and stress response in the 3xTg-AD mice. Neurobiol Dis. 2007;28:76-82.
24. Stover KR, Campbell MA, Van Winssen CM, Brown RE. Early detection of cognitive deficits in the 3xTg-AD mouse model of Alzheimer's disease. Behav Brain Res. 2015;289:29-38.
25. Thal DR, Rüb U, Orantes M, Braak H. Phases of A beta-deposition in the human brain and its relevance for the development of AD. Neurology. 2002;58:1791-1800.
26. Koffie RM, Hashimoto T, Tai HC, Kay KR, Serrano-Pozo A, Joyner D, et al. Apolipoprotein E4 effects in Alzheimer's disease are mediated by synaptotoxic oligomeric amyloid-β. Brain. 2012;135:2155-2168.
27. Jackson RJ, Rudinskiy N, Herrmann AG, Croft S, Kim JM, Petrova V, et al. Human tau increases amyloid β plaque size but not amyloid β-mediated synapse loss in a novel mouse model of Alzheimer's disease. Eur J Neurosci. 2016;44:3056-3066.
28. Ashe KH, Zahs KR. Probing the biology of Alzheimer's disease in mice. Neuron. 2010;66:631-645.
29. Sasaguri H, Nilsson P, Hashimoto S, Nagata K, Saito T, Strooper BD, et al. APP mouse models for Alzheimer's disease preclinical studies. EMBO J. 2017;36:2473-2487.
30. de Wilde MC, Overk CR, Sijben JW, Masliah E. Meta-analysis of synaptic pathology in Alzheimer's disease reveals selective molecular vesicular machinery vulnerability. Alzheimers Dement. 2016;12:633-644.
31. Heneka MT, Carson MJ, El Khoury J, Khoury JE, Landreth GE, Brosseron F, et al. Neuroinflammation in Alzheimer's disease. Lancet Neurol. 2015;14:388-405.
32. Hickman S, Izzy S, Sen P, Morsett L, El Khoury J. Microglia in neurodegeneration. Nat Neurosci. 2018;21:1359-1369.
33. Heppner FL, Ransohoff RM, Becher B. Immune attack: the role of inflammation in Alzheimer disease. Nat Rev Neurosci. 2015;16:358-372.
34. Pekny M, Pekna M, Messing A, Steinhauser C, Lee JM, Parpura V, et al. Astrocytes: a central element in neurological diseases. Acta Neuropathol. 2016;131:323-345.
35. Rodríguez-Arellano JJ, Parpura V, Zorec R, Verkhratsky A. Astrocytes in physiological aging and Alzheimer's disease. Neuroscience. 2016;323:170-182.
36. Choi BR, Cho WH, Kim J, Lee JH, Chung C, Jeon WK, et al. Increased expression of the receptor for advanced glycation end products in neurons and astrocytes in a triple transgenic mouse model of Alzheimer's disease. Exp Mol Med. 2014;46(2):e75.
37. Chen Y, Liang Z, Tian Z, Blanchare J, Dai CL, Chalbot S, et al. Intracerebroventricular streptozotocin exacerbates Alzheimer-like changes of 3xTg-AD mice. Mol Neurobiol. 2014;49:547-562.
38. Kim D, Cho J, Kang H. Protective effect of exercise training against the progression of Alzheimer's disease in 3xTg-AD mice. Behav Brain Res. 2019;374:112105.
39. Mosher KI, Wyss-Coray T. Microglial dysfunction in brain aging and Alzheimer's disease. Biochem Pharmacol. 2014;88:594-604.

40. Zhou L, Huang JY, Zhang D, Zhao YL. Cognitive improvements and reduction in amyloid plaque deposition by saikosaponin D treatment in a murine model of Alzheimer's disease. Exp Ther Med. 2020;20:1082-1090.
41. Bashiri H, Enayati M, Bashiri A, Salari AA. Swimming exercise improves cognitive and behavioral disorders in male NMRI mice with sporadic Alzheimer-like disease. Physiol Behav. 2020;223:113003.
42. Do K, Laing BT, Landry T, Bunner W, Mersaud N, Matsubara T, et al. The effects of exercise on hypothalamic neurodegeneration of Alzheimer's disease mouse model. PLoS One. 2018;13:e0190205.
43. Querfurth HW, LaFerla FM. Alzheimer's disease. N Engl J Med. 2010;362:329-344.
44. Lim D, Iyer A, Ronco V, Grolla AA, Canonico PL, Aronica E, et al. Amyloid beta deregulates astroglial mGluR5-mediated calcium signaling via calcineurin and Nf-kB. Glia. 2013;61:1134-1145.
45. Wood LB, Winslow AR, Proctor EA, McGuone D, Mordes DA, Frosch MP, et al. Identification of neurotoxic cytokines by profiling Alzheimer's disease tissues and neuron culture viability screening. Sci Rep. 2015;5:16622.
46. Wang W, Zhao F, Ma X, Perry G, Zhu X. Mitochondria dysfunction in the pathogenesis of Alzheimer's disease: recent advances. Mol Neurodegener. 2020;15:30.
47. Abramov AY, Canevari L, Duchen MR. Beta-amyloid peptides induce mitochondrial dysfunction and oxidative stress in astrocytes and death of neurons through activation of NADPH oxidase. J Neurosci. 2004;24:565-575.
48. Lustbader JW, Cirilli M, Lin C, Xu HW, Takuma K, Wang N, et al. ABAD directly links Abeta to mitochondrial toxicity in Alzheimer's disease. Science. 2004;304:448-452.
49. Chin JH, Tse FW, Harris K, Jhamandas JH. Beta-amyloid enhances intracellular calcium rises mediated by repeated activation of intracellular calcium stores and nicotinic receptors in acutely dissociated rat basal forebrain neurons. Brain Cell Biol. 2006;35:173-186.
50. Du H, Yan SS. Mitochondrial permeability transition pore in Alzheimer's disease: cyclophilin D and amyloid beta. Biochim Biophys Acta. 2010;1802:198-204.
51. Du H, Guo L, Fang F, Chen D, Sosunov AA, Mckhann GM, et al. Cyclophilin D deficiency attenuates mitochondrial and neuronal perturbation and ameliorates learning and memory in Alzheimer's disease. Nat Med. 2008;14:1097-1105.
52. Cuadrado-Tejedor M, Vilariño M, Cabodevilla F, Del Río J, Frechilla D, Pérez-Mediavilla A. Enhanced expression of the voltage-dependent anion channel 1 (VDAC1) in Alzheimer's disease transgenic mice: an insight into the pathogenic effects of amyloid-β. J Alzheimers Dis. 2011;23:195-206.
53. Singh P, Suman S, Chandna S, Das TK. Possible role of amyloid-beta, adenine nucleotide translocase and cyclophilin-D interaction in mitochondrial dysfunction of Alzheimer's disease. Bioinformation. 2009;3:440-445.
54. Manczak M, Anekonda TS, Henson E, Park BS, Quinn J, Reddy PH. Mitochondria are a direct site of A beta accumulation in Alzheimer's disease neurons: implications for free radical generation and oxidative damage in disease progression. Hum Mol Genet. 2006;15:1437-1449.

55. Opazo C, Huang X, Cherny RA, Moir RD, Roher AE, White AR, et al. Metalloenzyme-like activity of Alzheimer's disease beta-amyloid. Cu-dependent catalytic conversion of dopamine, cholesterol, and biological reducing agents to neurotoxic H(2)O(2). J Biol Chem. 2002;277:40302-40308.
56. Ruthel G, Hollenbeck PJ. Response of mitochondrial traffic to axon determination and differential branch growth. J Neurosci. 2003;23:8618-8624.
57. Sun T, Qiao H, Pan PY, Chen Y, Sheng ZH. Motile axonal mitochondria contribute to the variability of presynaptic strength. Cell Rep. 2013;:413-419.
58. Ye M, Chung HS, An YH, Lim SJ, Choi W, Yu AR, et al. Standardized Herbal Formula PM012 Decreases Cognitive Impairment and Promotes Neurogenesis in the 3xTg AD Mouse Model of Alzheimer's Disease. Mol Neurobiol. 2016;53:5401-5412.
59. Hu Y, Lai J, Wan B, Liu Z, Zhang Y, Zhang J, et al. Long-term exposure to ELF-MF ameliorates cognitive deficits and attenuates tau hyperphosphorylation in 3xTg AD mice. Neurotoxicology. 2016;53:290-300.
60. Hedberg MM, Clos MV, Ratia M, Gonzalez D, Lithner CU, Camps P, et al. Effect of huprine X on β-amyloid, synaptophysin and α7 neuronal nicotinic acetylcholine receptors in the brain of 3xTg-AD and APPswe transgenic mice. Neurodegener Dis. 2010;7:379-388.
61. Shruster A, Offen D. Targeting neurogenesis ameliorates danger assessment in a mouse model of Alzheimer's disease. Behav Brain Res. 2014;261:193-201.
62. Prakash A, Kumar A. Role of nuclear receptor on regulation of BDNF and neuroinflammation in hippocampus of β-amyloid animal model of Alzheimer's disease. Neurotox Res. 2014;25:335-347.
63. Peng S, Wuu J, Mufson EJ, Fahnestock M. Precursor form of brain-derived neurotrophic factor and mature brain-derived neurotrophic factor are decreased in the pre-clinical stages of Alzheimer's disease. J Neurochem. 2005;93:1412-1421.
64. Moreno-Jiménez EP, Flor-García M, Terreros-Roncal J, Rabano A, Cafini F, Pallas-Bazarra N, et al. Adult hippocampal neurogenesis is abundant in neurologically healthy subjects and drops sharply in patients with Alzheimer's disease. Nat Med. 2019;25:554-560.
65. Tobin MK, Musaraca K, Disouky A, Shetti A, Bheri A, Honer WG, et al. Human Hippocampal Neurogenesis Persists in Aged Adults and Alzheimer's Disease Patients. Cell Stem Cell. 2019;24:974-982.
66. Qin XY, Cao C, Cawley NX, Liu TT, Yuan J, Loh YP, et al. Decreased peripheral brain-derived neurotrophic factor levels in Alzheimer's disease: a meta-analysis study (N=7277). Mol Psychiatry. 2017;22(2):312-320.
67. Palop JJ, Chin J, Roberson ED, Wang J, Thwin MT, Ly B, et al. Aberrant excitatory neuronal activity and compensatory remodeling of inhibitory hippocampal circuits in mouse models of Alzheimer's disease. Neuron. 2007;55:697-711.
68. Stam CJ, van Cappellen van Walsum AM, Pijnenburg YA, Berendse HW, de Munck JC, Scheltens P, et al. Generalized synchronization of MEG recordings in Alzheimer's Disease: evidence for involvement of the gamma band. J Clin Neurophysiol. 2002;19:562-574.

69. Verret L, Mann EO, Hang GB, Barth AMI, Cobos I, Ho K, et al. Inhibitory interneuron deficit links altered network activity and cognitive dysfunction in Alzheimer model. Cell. 2012;149:708-721.
70. Gillespie AK, Jones EA, Lin YH, Karlsson MP, Kay K, Yoon SY, et al. Apolipoprotein E4 Causes Age-Dependent Disruption of Slow Gamma Oscillations during Hippocampal Sharp-Wave Ripples. Neuron. 2016;90:740-751.
71. Klein AS, Donoso JR, Kempter R, Schmitz D, Beed P. Early Cortical Changes in Gamma Oscillations in Alzheimer's Disease. Front Syst Neurosci. 2016;10:83.
72. Kurudenkandy FR, Zilberter M, Biverstål H, Presto J, Honcharenko D, Strömberg R, et al. Amyloid-β-induced action potential desynchronization and degradation of hippocampal gamma oscillations is prevented by interference with peptide conformation change and aggregation. J Neurosci. 2014 Aug 20;34:11416-25.
73. Whittaker RG, Turnbull DM, Whittington MA, Cunningham MO. Impaired mitochondrial function abolishes gamma oscillations in the hippocampus through an effect on fast-spiking interneurons. Brain. 2011;134:e180-181.
74. Goutagny R, Gu N, Cavanagh C, Jackson J, Chabot JG, Quirion R, et al. Alterations in hippocampal network oscillations and theta-gamma coupling arise before Aβ overproduction in a mouse model of Alzheimer's disease. Eur J Neurosci. 2013;37(12):1896-1902.
75. Adaikkan C, Middleton SJ, Marco A, Pao PC, Mathys H, Kim DNW, et al. Gamma Entrainment Binds Higher-Order Brain Regions and Offers Neuroprotection. Neuron. 2019;102:929-943.e8.
76. Cass SP. Alzheimer's Disease and Exercise: A Literature Review. Curr Sports Med Rep. 2017;16:19-22.
77. García-Mesa Y, López-Ramos JC, Giménez-Llort L, Revila S, Guerra R, Gurart A, et al. Physical exercise protects against Alzheimer's disease in 3xTg-AD mice. J Alzheimers Dis. 2011;24:421-454.
78. Brown BM, Peiffer JJ, Taddei K, Laws SM, Gupta VB, Taddei T, et al. Physical activity and amyloid-β plasma and brain levels: results from the Australian Imaging, Biomarkers and Lifestyle Study of Ageing. Mol Psychiatry. 2013;18:875-881.
79. Brown BM, Sohrabi HR, Taddei K, Gardener SL, Rainey-Smith SR, Peiffer J, et al. Habitual exercise levels are associated with cerebral amyloid load in presymptomatic autosomal dominant Alzheimer's disease. Alzheimers Dement. 2017;13:1197-1206.
80. Radak Z, Hart N, Sarga L, Koltai E, Atalay M, Ohno H, et al. Exercise plays a preventive role against Alzheimer's disease. J Alzheimers Dis. 2010;20(3):777-783.
81. Liu Y, Chu JMT, Yan T, Zhang Y, Chen Y, Chang RCC, et al. Short-term resistance exercise inhibits neuroinflammation and attenuates neuropathological changes in 3xTg Alzheimer's disease mice. J Neuroinflammation. 2020;17:4.
82. Kim D, Cho J, Kang H. Protective effect of exercise training against the progression of Alzheimer's disease in 3xTg-AD mice. Behav Brain Res. 2019;374:112105.
83. Leem YH, Lee YI, Son HJ, Lee SH. Chronic exercise ameliorates the neuroinflammation in mice carrying NSE/htau23. Biochem Biophys Res Commun. 2011;406:359-365.

84. Marques-Aleixo I, Santos-Alves E, Balça MM, Roca-Rizo D, Moreira PI, Magalhaes J, et al. Physical exercise improves brain cortex and cerebellum mitochondrial bioenergetics and alters apoptotic, dynamic and auto(mito)phagy markers. Neuroscience. 2015;301:480-495.
85. Seo JH, Park HS, Park SS, Kim CJ, Kim DH, Kim TW. Physical exercise ameliorates psychiatric disorders and cognitive dysfunctions by hippocampal mitochondrial function and neuroplasticity in post-traumatic stress disorder. Exp Neurol. 2019;322:113043.
86. Um HS, Kang EB, Koo JH, Kim HT, Lee J, Kim EJ, et al. Treadmill exercise represses neuronal cell death in an aged transgenic mouse model of Alzheimer's disease. Neurosci Res. 2011;69:161-173.
87. Baek SS, Kim SH. Treadmill exercise ameliorates symptoms of Alzheimer disease through suppressing microglial activation-induced apoptosis in rats. J Exerc Rehabil. 2016;12:526-534.
88. Markham A, Cameron I, Franklin P, Spedding M. BDNF increases rat brain mitochondrial respiratory coupling at complex I, but not complex II. Eur J Neurosci. 2004;20:1189-1196.
89. Gómez-Pinilla F, Ying Z, Roy RR, Molteni R, Edgerton VR. Voluntary exercise induces a BDNF-mediated mechanism that promotes neuroplasticity. J Neurophysiol. 2002;88:2187-2195.
90. Adlard PA, Perreau VM, Cotman CW. The exercise-induced expression of BDNF within the hippocampus varies across life-span. Neurobiol Aging. 2005;26:511-520.
91. Kovalchuk Y, Hanse E, Kafitz KW, Konnerth A. Postsynaptic Induction of BDNF-Mediated Long-Term Potentiation. Science. 2002;295:1729-1734.
92. Martin JL, Finsterwald C. Cooperation between BDNF and glutamate in the regulation of synaptic transmission and neuronal development. Commun Integr Biol. 2011;4:14-16.
93. Cho J, Shin MK, Kim D, Lee I, Kim S, Kang H. Treadmill Running Reverses Cognitive Declines due to Alzheimer Disease. Med Sci Sports Exerc. 2015;47:1814-1824.
94. Revilla S, Suñol C, García-Mesa Y, Giménez-Llort L, Sanfeliu C, Cristòfol R. Physical exercise improves synaptic dysfunction and recovers the loss of survival factors in 3xTg-AD mouse brain. Neuropharmacology. 2014;81:55-63.
95. Choi SH, Bylykbashi E, Chatila ZK, Lee SW, Pulli B, Clemenson GD, et al. Combined adult neurogenesis and BDNF mimic exercise effects on cognition in an Alzheimer's mouse model. Science. 2018;361:eaan8821.

# Figures

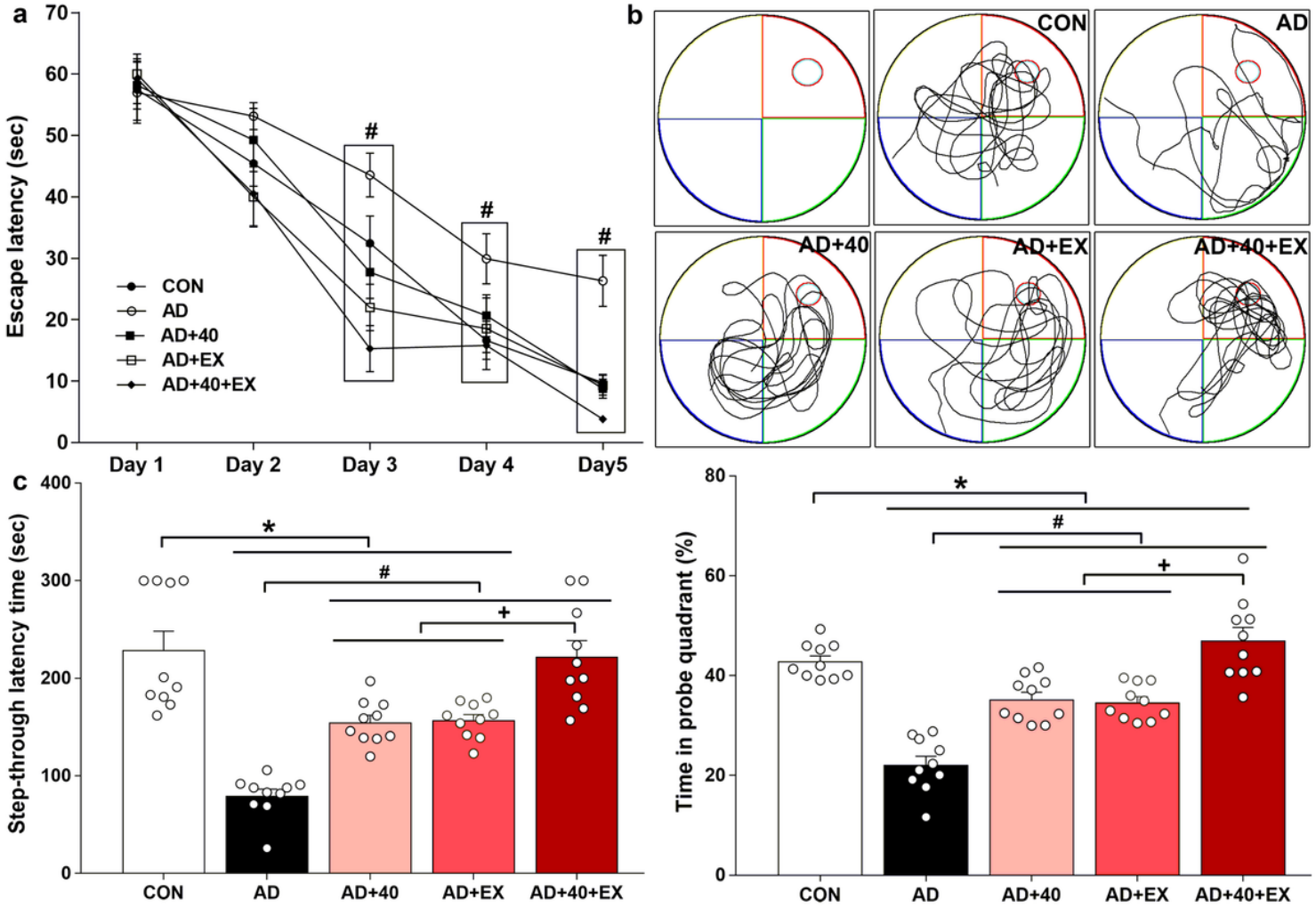


## Figure 1

Effects of exercise under exposure to 40-Hz light flicker on spatial learning (a) and memory (b) and long-term memory (c) in the AD. The Morris water maze task was used to evaluate spatial learning and memory and step-through task was used for long-term memory. CON: non-transgenic, AD: 3xTg-AD, AD+40: 3xTg-AD and 40-Hz light flickering AD+EX: 3xTg-AD and exercise, AD+40+EX: 3xTg-AD and exercise with 40-Hz light flickering. Data are expressed as means ± standard error of the mean (SEM). *p < 0.05 compared to the CON group. # p < 0.05 compared to the AD group. + p < 0.05 compared to the AD+40+EX group.

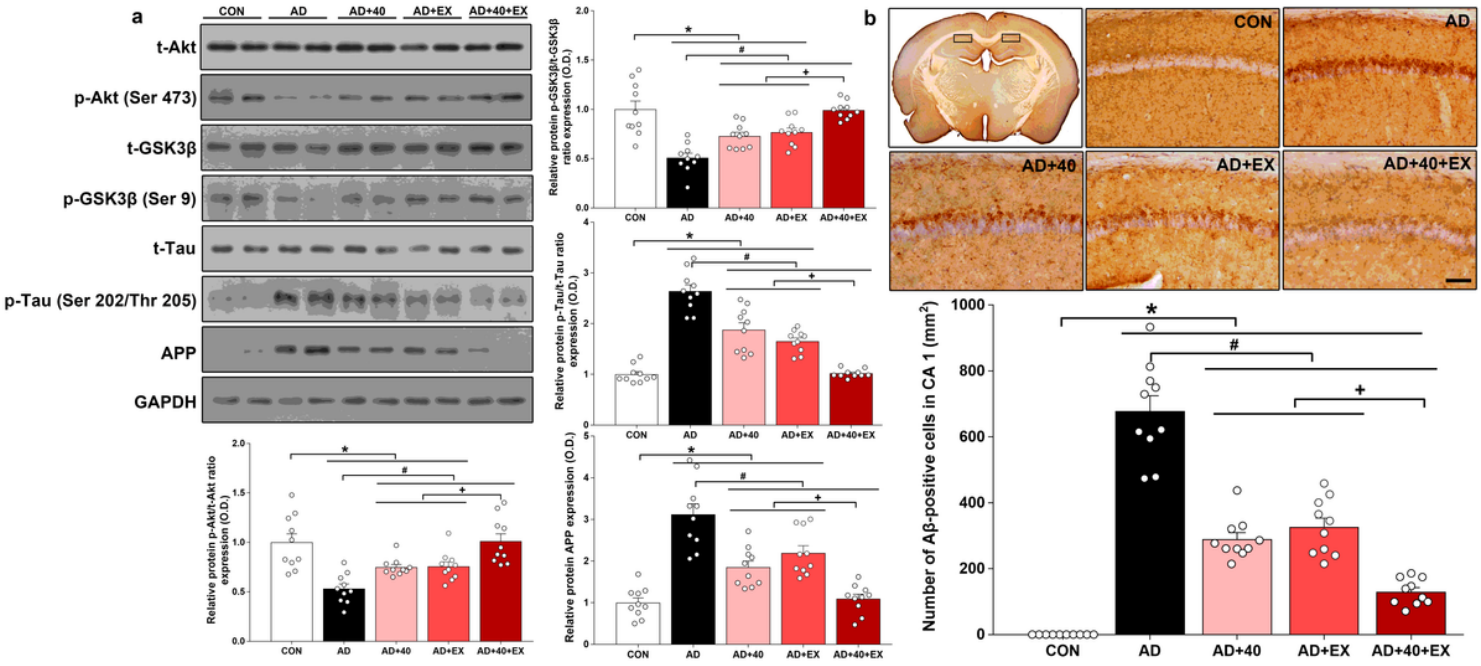


## Figure 2

Effects of exercise under exposure to 40-Hz light flicker on the p-Akt/t-Akt, p-GSK3β/t-GSK3β, and p-tau/t-tau ratios in the hippocampus (a) and Aβ in hippocampal CA1 (b) of AD. Representative photomicrographs and data for Aβ-positive cells are shown. The scale bar represents 50 μm. CON: non-transgenic, AD: 3xTg-AD, AD+40: 3xTg-AD and 40-Hz light flickering AD+EX: 3xTg-AD and exercise, AD+40+EX: 3xTg-AD and exercise with 40-Hz light flickering. Data are expressed as means ± standard error of the mean (SEM). *p < 0.05 compared to the CON group. # p < 0.05 compared to the AD group. + p < 0.05 compared to the AD+40+EX group.

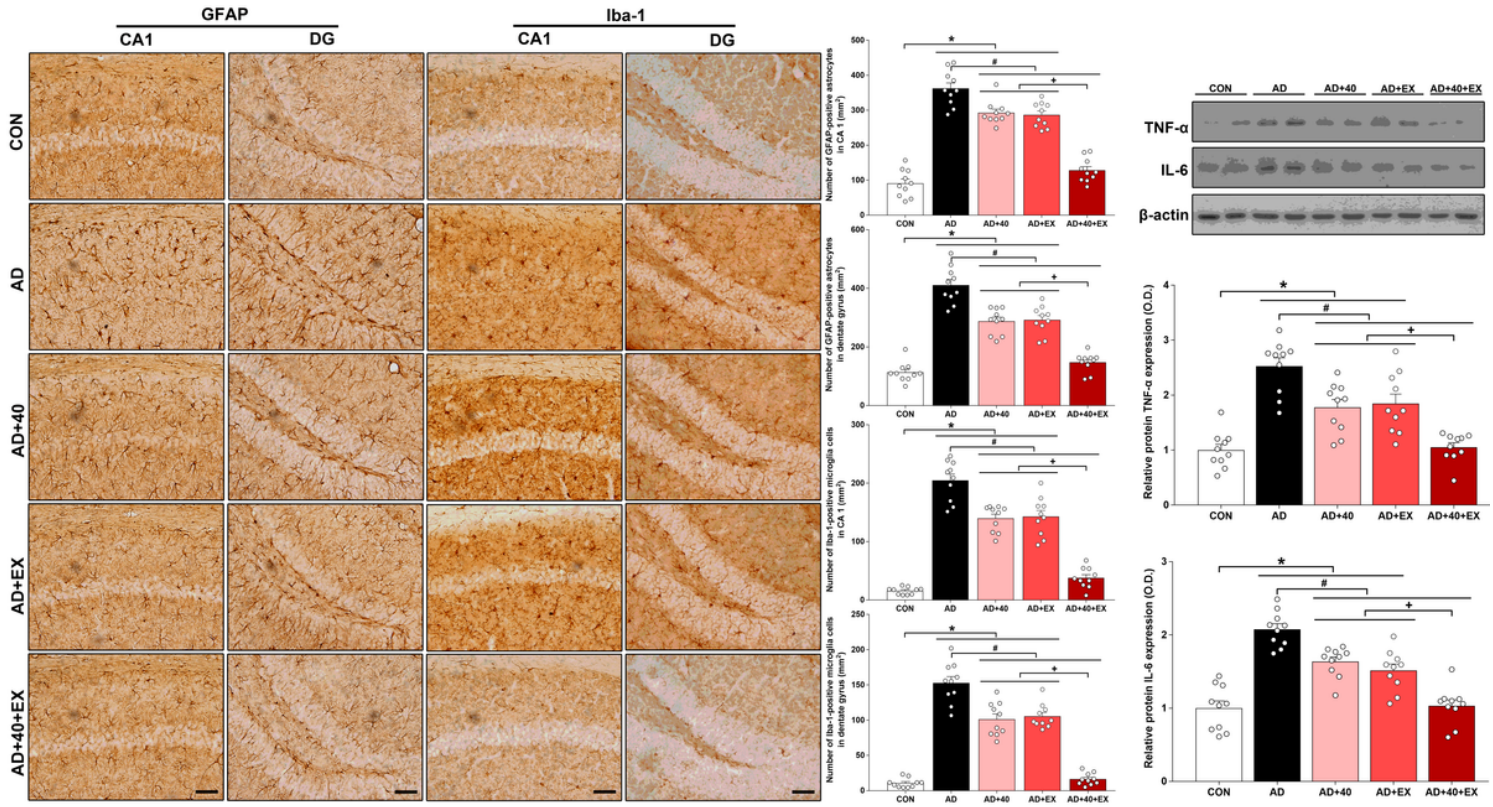


## Figure 3

Effects of exercise under exposure to 40-Hz light flicker on neuroinflammation in the hippocampal CA1 and DG and pro-inflammatory cytokines in the hippocampus of AD. Representative photomicrographs and data for GFAP-positive astrocytes and Iba-1-positive microglial cells are shown. The scale bar represents 50 μm. CON: non-transgenic, AD: 3xTg-AD, AD+40: 3xTg-AD and 40-Hz light flickering AD+EX: 3xTg-AD and exercise, AD+40+EX: 3xTg-AD and exercise with 40-Hz light flickering. Data are expressed as means ± standard error of the mean (SEM). * $p < 0.05$ compared to the CON group. # $p < 0.05$ compared to the AD group. + $p < 0.05$ compared to the AD+40+EX group.

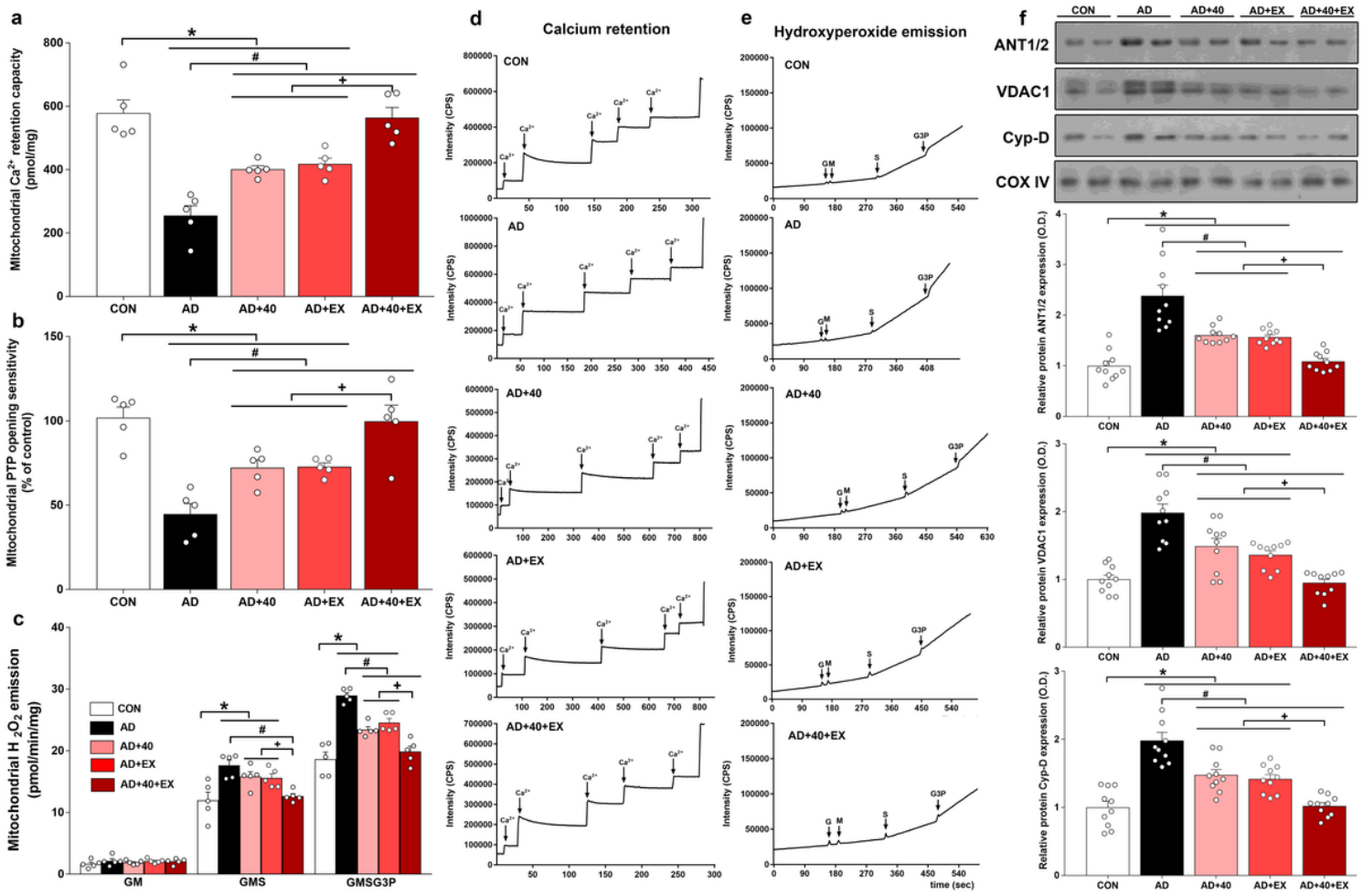


## Figure 4

Effects of exercise under exposure to 40-Hz light flicker on mitochondrial Ca2+ retention (a), H2O2 emission (b), and mPTP-related protein expression (f) in the hippocampus of AD. The total mitochondrial Ca2+ retention capacity prior to PTP opening (i.e., release of Ca2+) was determined. Ca2+↓ indicates Ca2+ infusion in calcium retention (d). G↓ indicates glutamate infusion; M↓ indicates malate infusion; S↓, succinate infusion; G3P↓ indicates glycerol-3-phosphate infusion in hydroxyperoxide emission (e). CON: non-transgenic, AD: 3xTg-AD, AD+40: 3xTg-AD and 40-Hz light flickering AD+EX: 3xTg-AD and exercise, AD+40+EX: 3xTg-AD and exercise with 40-Hz light flickering. Data are expressed as means ± standard error of the mean (SEM). * $p < 0.05$ compared to the CON group. # $p < 0.05$ compared to the AD group. + $p < 0.05$ compared to the AD+40+EX group

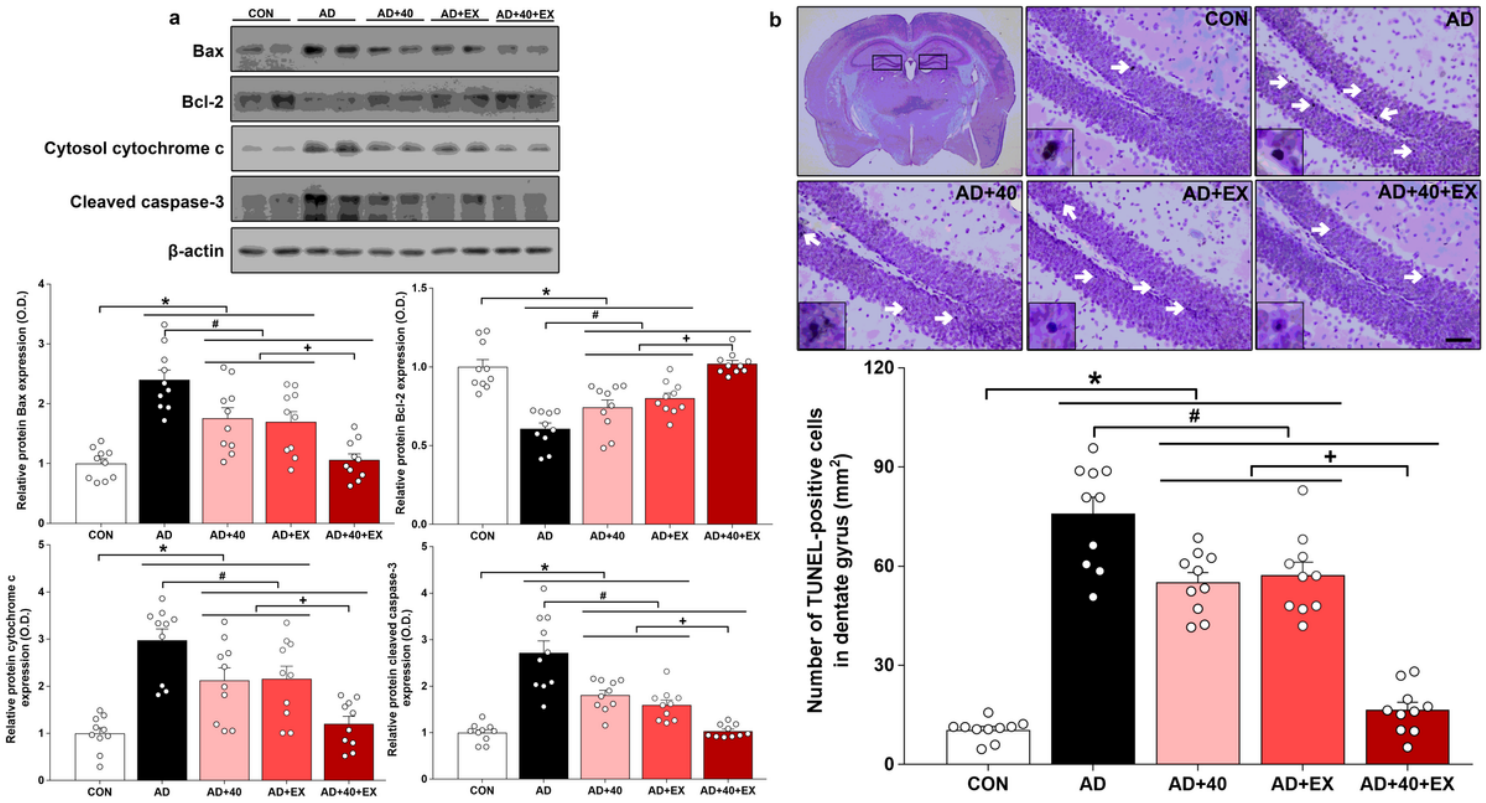


## Figure 5

Effects of exercise under exposure to 40-Hz light flicker on apoptosis (a) and cell death (b) in the hippocampus of AD. Representative photomicrographs and data for TUNEL-positive cells are shown. The scale bar represents 50 μm. CON: non-transgenic, AD: 3xTg-AD, AD+40: 3xTg-AD and 40-Hz light flickering AD+EX: 3xTg-AD and exercise, AD+40+EX: 3xTg-AD and exercise with 40-Hz light flickering. Data are expressed as means ± standard error of the mean (SEM). * $p < 0.05$ compared to the CON group. # $p < 0.05$ compared to the AD group. + $p < 0.05$ compared to the AD+40+EX group.

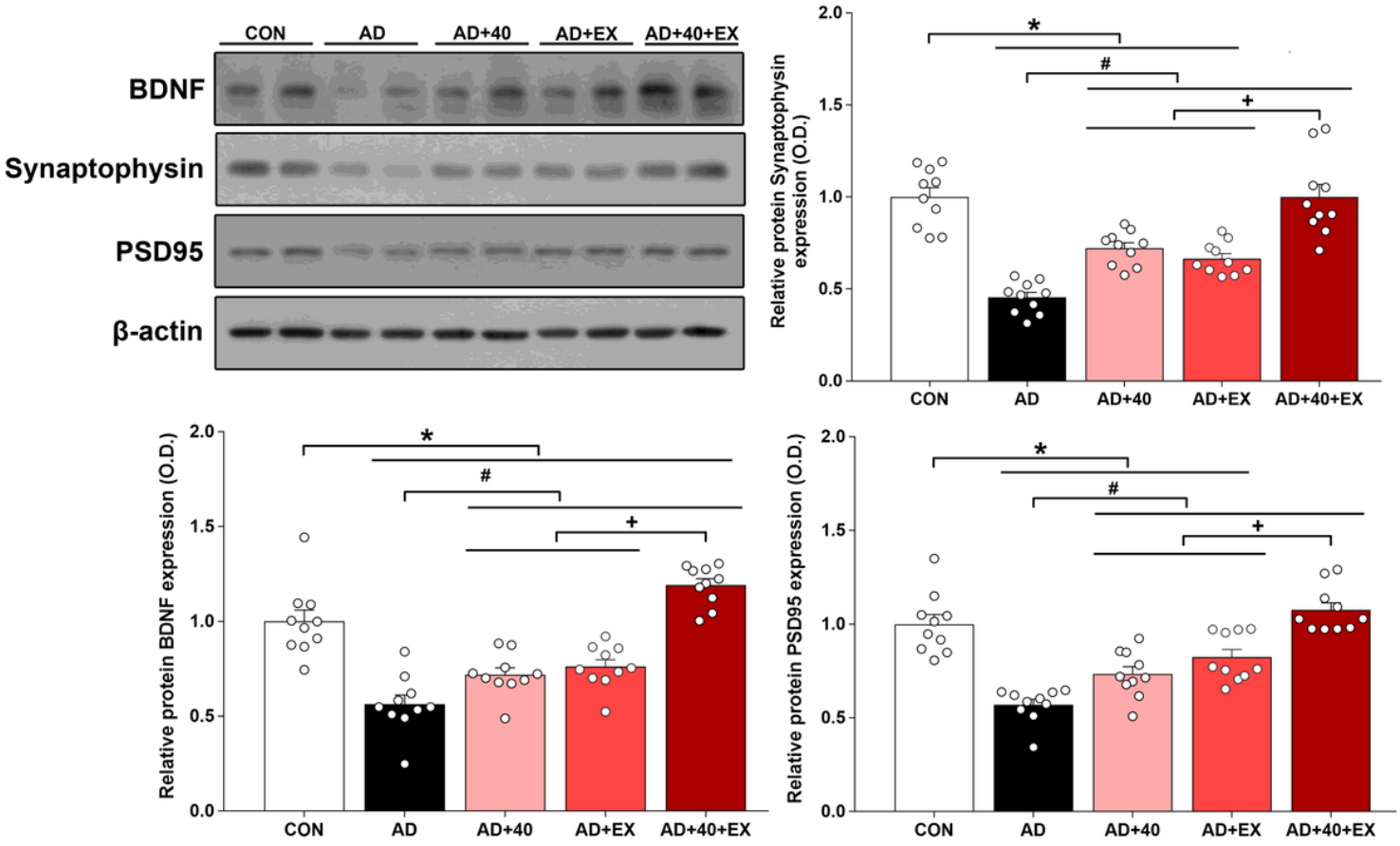


## Figure 6

Effects of exercise under exposure to 40-Hz light flicker on BDNF, synaptophysin, and PSD95 in the hippocampus of AD. CON: non-transgenic, AD: 3xTg-AD, AD+40: 3xTg-AD and 40-Hz light flickering AD+EX: 3xTg-AD and exercise, AD+40+EX: 3xTg-AD and exercise with 40-Hz light flickering. Data are expressed as means ± standard error of the mean (SEM). * $p < 0.05$ compared to the CON group. # $p < 0.05$ compared to the AD group. + $p < 0.05$ compared to the AD+40+EX group.

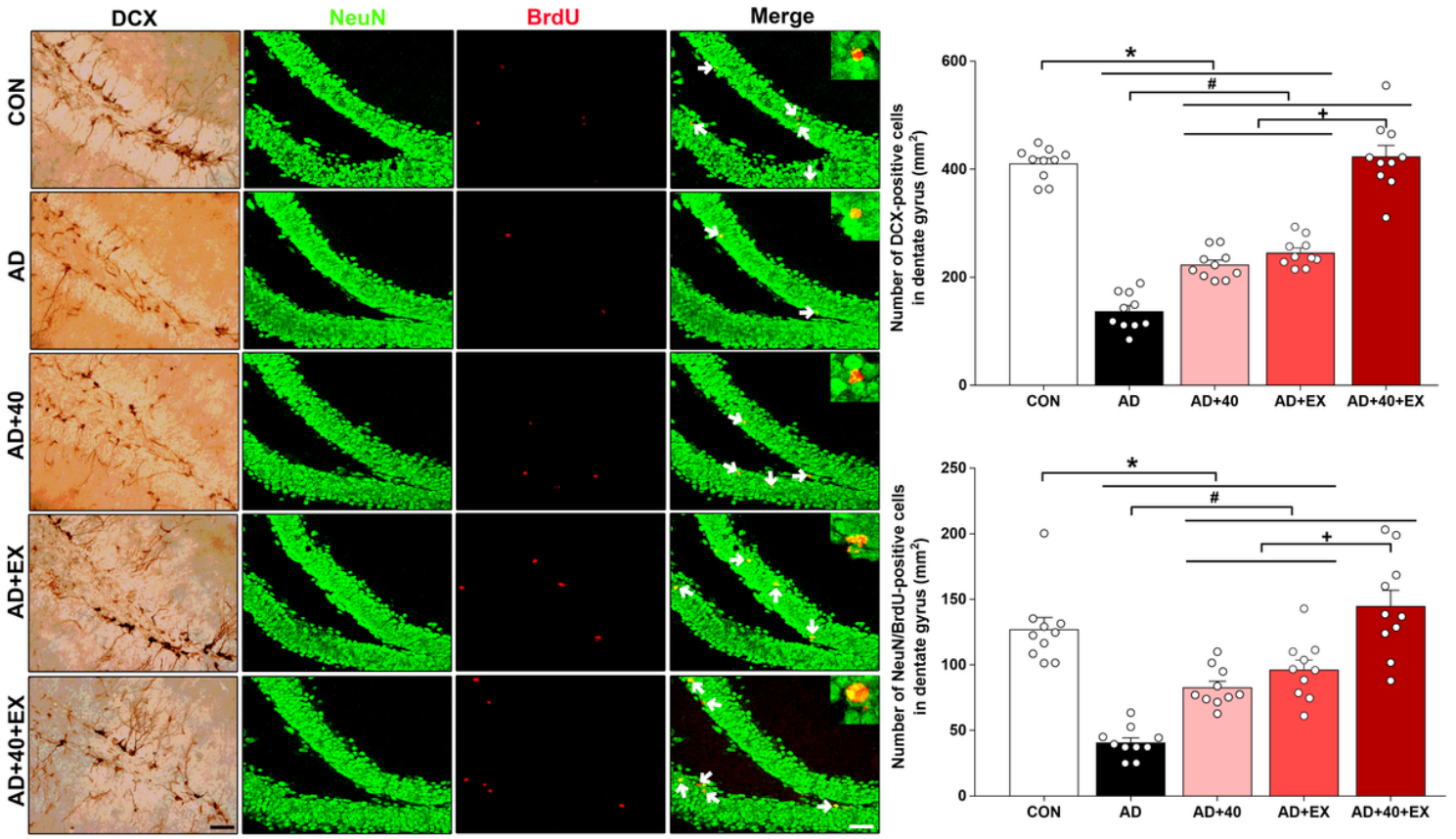


## Figure 7

Effects of exercise under exposure to 40-Hz light flicker on cell differentiation and neurogenesis in the hippocampal dentate gyrus of AD. Representative photomicrographs and data for DCX- and NeuN/BrdU-positive cells are shown. The scale bar represents 50 μm. CON: non-transgenic, AD: 3xTg-AD, AD+40: 3xTg-AD and 40-Hz light flickering AD+EX: 3xTg-AD and exercise, AD+40+EX: 3xTg-AD and exercise with 40-Hz light flickering. Data are expressed as means ± standard error of the mean (SEM). * $p < 0.05$ compared to the CON group. # $p < 0.05$ compared to the AD group. + $p < 0.05$ compared to the AD+40+EX group.